THE DEVELOPEMENT OF RED MUD FLOOD ENVIRONMENTAL INFORMATION SYSTEM AND THE METHODOLOGY FOR THE SPATIAL ANALYSIS OF THE DEGRADED AREA

GÁBOR BAKÓ[1]*, GÁBOR KOVÁCS[2], ZSOLT MOLNÁR[3], JUDIT KIRISICS[4], ESZTER GÓBER[5], ANDRÁS AMBRUS[6]

[1]Institute of Botany and Ecophysiology, Szent István University, Gödöllő, H-2100 Gödöllő Páter K. u. 1., Hungary
E-mail: info@interspect.hu
[2]Department of Geophysics and Space Science, Eötvös University, Budapest, Hungary
[1, 3, 5]Remote Sensing Branch, Interspect Research Group, Halásztelek, Hungary
[4, 6]Department of Cartography and Geoinformatics, Eötvös University, Budapest, Hungary
* corresponding author

Received 15 March 2015, accepted in revised form 4 May 2015

Abstract
The red mud disaster occurred on 4th October 2010 in Hungary has raised the necessity of rapid intervention and drew attention to the long-term monitoring of such threat. Both the condition assessment and the change monitoring indispensably required the prompt and detailed spatial survey of the impact area. It was conducted by several research groups - independently - with different recent surveying methods. The high spatial resolution multispectral aerial photogrammetry is the spatially detailed (high resolution) and accurate type of remote sensing. The hyperspectral remote sensing provides more information about material quality of pollutants, with less spatial details and lower spatial accuracy, while LIDAR ensures the three-dimensional shape and terrain models. The article focuses on the high spatial resolution, multispectral electrooptical method and the evaluation methodology of the deriving high spatial resolution ortho image map, presenting the derived environmental information database.

Keywords: remote sensing, risk management, aerial photogrammetry, red mud disaster, aerial instruments, classification, image segmentation, damage assessment and mapping, landscape ecology

1. Introduction

The corrective measures of disaster recovery and the preventive study of hazardous areas require efficient, highly detailed, GIS-based decision-support system. Environmental databases help the systematization of the spot collected information provided by on-site sampling and the surface data obtained from remote sensing. GIS applications based on these databases promote disaster recovery planning and evaluation of the environmental effects. Furthermore, they provide a statistical comparison of test data and facilitate the extraction of spatial model inputs by easily interpreted thematic maps. Nowadays, the ecological models are usually based on information summarized by the Environmental Information System based on GIS layers of the surface analysis.

The survey of the area was urgent for the defence. As it appeared on the Hungarian Academy of Sciences webpage: 'The environmental damage, especially soil contamination, affects a well-defined area. The organized prevention of further damage takes place on a continuous basis' (MTA.hu, 2011). The direct impact area of the disaster occurred in October 2010 has been investigated at the same time of our survey

Fig. 1. The reservoir on 06th October 2010

by different remote sensing methods. During data collection, five different remote sensing systems were used and the processing of different technologies and the collected data were intended to be streamlined and combined for both short- and long-term purposes. The approximate size of the affected area was estimated at about 1,000 ha based on the information derived from the high spatial resolution IKONOS satellite data (GeoEye) and airborne imagery (Disaster Management) (Burai et al., 2011). Our aim was to create a database with high accuracy by increasing the spatial resolution and applying the new generation CMOS sensors (Bakó, 2012) which is more detailed than databases of space remote sensing or low-resolution aerial remote sensing. Similarly to the segment-based classification solutions of aerial and satellite images (László et al., 2011), we have also developed a methodology description for semi-automatic classification of our high-resolution orthophoto map accrued by aerial remote sensing.

The Red Mud Disaster

On 4th October 2010 at 12:05 pm (CET) the northwestern corner of red mud reservoir number X – where the maximum of shear stress concentrated – near Kolontár settlement (Hungary) has cracked and broke (Fig. 1.). The rapidly flowing red mud flood affected the inner area of Kolontár and Devecser (Fig. 2.) causing injury to 150 people and killing 10 people. Outside of the inhabited areas the catastrophe has caused significant damages in wildlife (Fig. 3.). Most of the casualties have been suffered first or second degree burns caused by the alkaline ingredients of the mud flow.

The flood reached seven settlements situated along the valley of Torna Stream. The channel was not wide enough to lead the mud without flooding the low-lying areas around. The contamination reached the River Danube, through the tributaries of Marcal, the Rába and the Moson-Danube rivers (Fig. 4.).

Immediately after the subside of the flood, 100 000 liters of alkaline water stored in the neighboring reservoir has been neutralized by using acid. After that, the cleaning of the Torna stream has begun by draining away the content of the older reservoir. Red mud is a hazardous solid waste product of refining bauxite containing minerals insoluble by natron and solid salts formed by compounds reactable with alkali.

Fig. 2. The personal belongings were taken away from the houses by the mud flood through the windows

The waste is produced by the extraction of alumina from bauxite ore in the Bayer process (Pulford et al., 2012). Like most of concentrated residues, the red mud contains some enriched radioactive elements too (Bálintné et al., 2012).

Fig. 3. The disaster damaged the wildlife as well: this dead fish was 10 meters from Torna Stream. Deer footprints in the red mud

1.5-2 tons of red mud is produced from 1 ton alumina production. The immediate impact was the devastation caused by the massive mud flood and its extremely high alkaline pH, in addition the indirect threat is the floating dust (Viczián, 2004). Experiments have shown that the Na salinity, not the trace metal contamination, is the main concern for this red mud in soil (Ruyters et al., 2011).

The red color of the mud is caused by the high concentration of ferric oxide. The alkalinity is a consequence of the high NaOH content, thus the untreated red mud is reckoned as hazardous, although EWC 01 03 09 is not determined as dangerous waste by European Union's legislation (Kátai et al., 2010). In nature, alkali by itself has no long-term environmental impact, because water dilutes it, however, in short-term it's corrosive effect causes vegetation damage (kvvm.hu, 2011). One of the major concerns about the aftermaths of the accident is the potential health effects of vast amounts of fugitive dust from red mud sediment. The University of Pannonia, Veszprém studied the chemical and physical properties of the red mud particles and dust; the scientists concluded that particles of red mud dust were too large to be inhaled deeply into lungs, where they could cause the most damage (Gelencsér et al., 2011).

2. Method

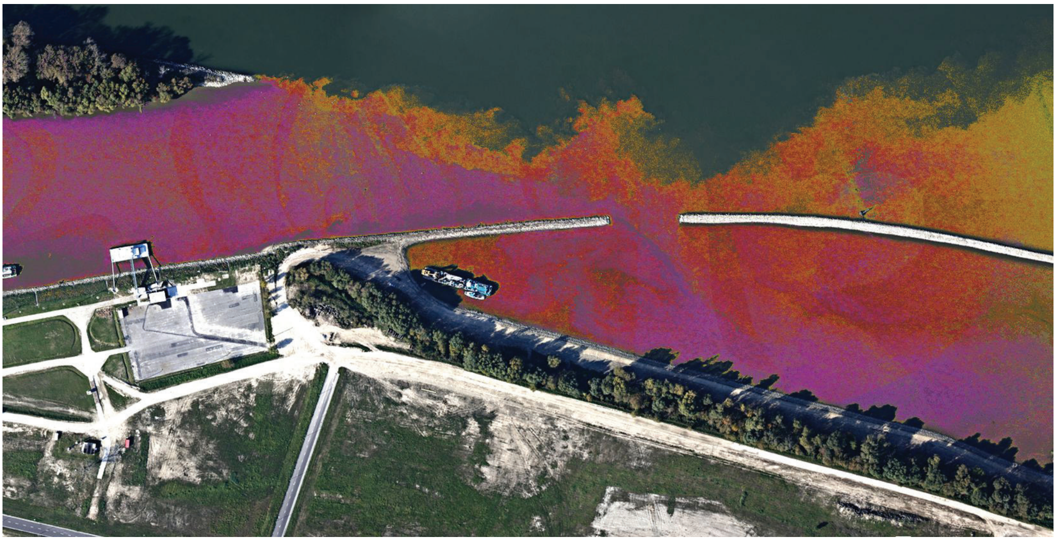

Fig. 4. On 11th October 2010 the contaminated water discharged into the Danube. Classified aerial map section. The dark purple indicates higher, yellow-green indicates lower contamination concentration

The Photogrammetric Survey that Substantiates the System

The order for mapping the affected area has arrived on 5th October from the Hungarian Ministry of Rural Development. The most efficient, rapidly productable base map to accurately locate the contaminated area and to plan recovery is the precisely georeferenced, high resolution aerial image-mosaic. The adverse weather permitted the survey of the entire area only on 6th October. To trace the effects of the contamination we planned time-series recording. The second survey conducted between 12:54 and 14:04 on 11th October has already detected the final-state of the red mud coverage. The high resolution survey has been performed by a plane expressly modified for remote sensing (Fig. 5.), from 1500 and 600 m relative flight altitude with own-developed IS 2 camera system. The acquired 300 perpendicular axes aerial images with 18 cm spatial resolution was the base of the 1:2100 scale aerial image map product. The high resolution georeferenced (Hungarian National Grid) images have been completed with oblique axis overview image series prepared from all sides, covering the whole area. After recording the directly affected area, the team surveyed the state of the contaminated river sections along the Torna Stream and Duna River towards Esztergom. The third, 11 cm-spatial resolution survey was conducted on 27th September 2011 from 1467 m relative flight altitude.

Fig. 5. Rapid preparation of an airplane is on the alert

Creation of accurate map required the collection of ground control points (GCPs). During a one week long fieldwork, the team collected 421 GCPs with 1.5 cm horizontal and 5 cm vertical accuracy (Fig. 6) for ortho-rectification and for accuracy analysis. These points in addition to the calibration data of camera system were necessary to process the true color (RGB) and multispectral images , correct distortions and georeference them.

The high spatial resolution is the base

of the high topographic accuracy, and our aim was to produce more accurate map than the available satellite images and the hyperspectral aerial mission. If the spatial resolution is higher, the GCPs can be identified more precisely. The surveying speed (ground speed of the flight) and the spatial resolution of our products are not the only development that makes them better than previous topographic maps and other aerial and satellite surveys; their density, hues also offers substantially wider range of visual interpretation and classification methods as (Fig. 7.) illustrates.

Fig. 6. Fieldwork on the contaminated area using geodetic GPS

Evaluation

The evaluation of the digital map has lasted two months for the Interspect Research Group due to the lack of financial support. The visual interpretation and the supervised classification have been carried out as interdisciplinary survey by experts. Our aim was to extract the changes of the buildings, the vegetation and the soil. The adequacy of area-based interpretation depends on the geometric accuracy and resolution of the image-map, as well as the accuracy of derived data of thematic interpretation (distortions and failures of visual and classification interpretation of the aerial maps, adequate joint of field data). Therefore the evaluation with thoroughly checked conditions accompanied by field controlling is crucial (Bakó, 2010). The georeferenced image-mosaic was especially useful for the disaster management, for the ministries and the universities that took part in the evaluation process. The time-series images record the changes in building stocks, vegetation, wildlife as well as soil- and water-quality. Using them the long-term environmental effects can be deducted.

Analysis of the Affected Area by Using Image Processing Methods

Firstly, the aim was the extraction of the red mud-covered areas by using classification,

Fig. 7. Google Earth section is on the left while on the right the aerial image made with IS 2 system is presenting the same area reduced to the same resolution

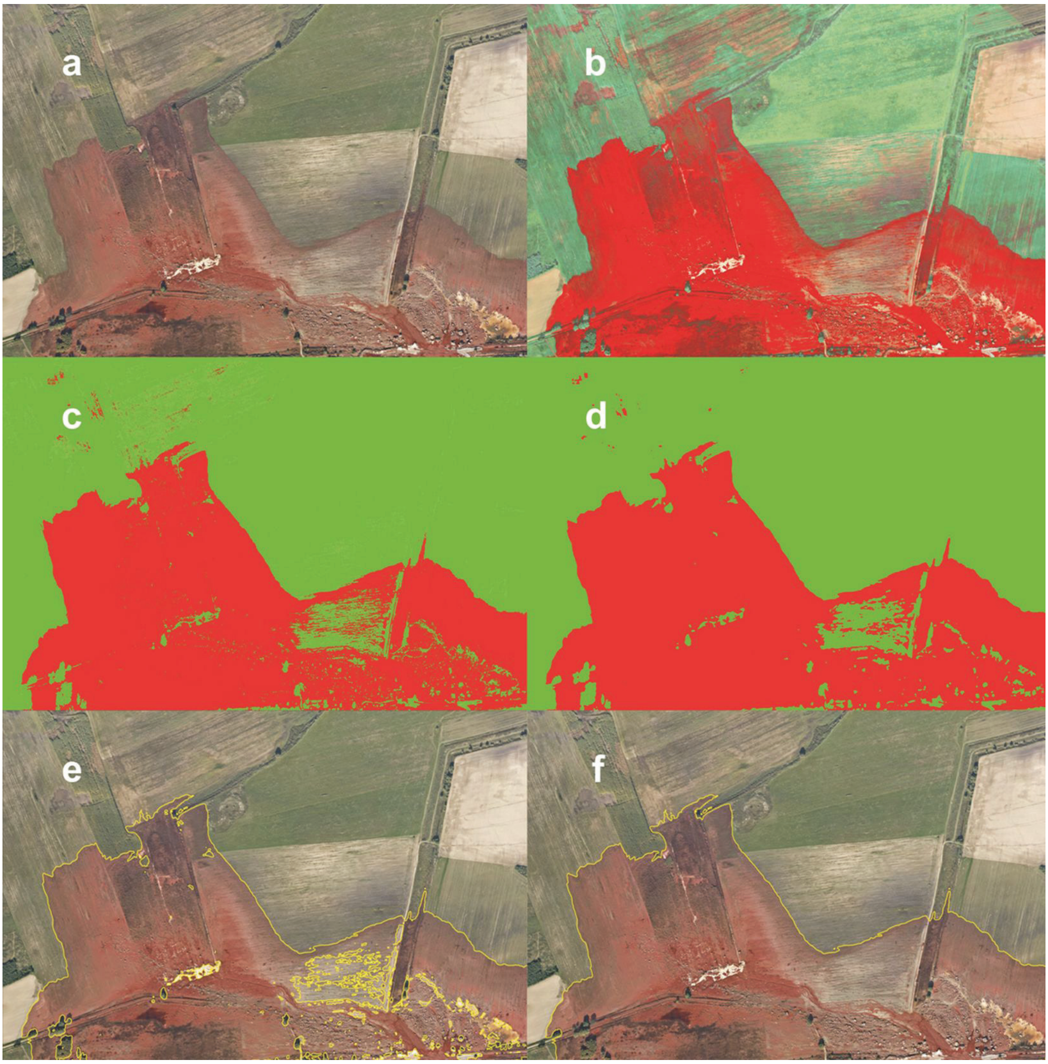

Fig. 8. Steps of the image processing: a) Section of the original aerial image map, b) Pre-classification, c) Classification, d) Dust filter, e) Vectorization, f) Correction

the vectorization of the red areas from the raster files, making land cover statistics and comparing these with the results of the visual interpretation.

Pre-Classification: Enhancement of the Red-Colored Areas.

The hue which corresponds to the red mud has been enhanced; this is how the images were prepared for a better segmentation.

The separation of the mud (from its surroundings) coverage was achieved by the configuratinghe features of the raster image like the selective colors. In case of the red component: reduction of the magenta and the cyan component, increasing of the red color; in case of the yellow component: increasing of the cyan, reduction of the magenta and yellow colors; in case of green and cyan component: radical decreasing of the cyan, magenta, yellow colors; in case of blue and magenta component: increasing of the yellow color.

In this way the surrounding land cover categories get fused. The color intensity of the orthophoto mosaic was radically changed, the hues were arranged, and the saturation was increased. The value of the blue channel's histogram was given as 0.01. In this way the mud-covered spots were significantly separated from their surroundings.

Classification

The supervised classification was processed by using ENVI 4.8 software. Two types of training area was defined and marked as regions of interest: one was red mud-covered, the other regions were not flooded.

The Minimum Distance method was found being the optional one, because the flooded regions were well-separated. The distance-based method is established, fast and responsible results can be expected. In this case, the base of the classification decision is the distance between the unknown pixel and the class average calculated for all thematic class samples. So the n-dimension point how far from is the centroid of the classes. The algorithm finds training area's average (per band) is the closest to the pixel's color.

This method results in a raster file in which the surfaces have homogeneous values, the pixels can get only two values. In the post-classification too small surfaces (<4 m2) were filtered; then these were merged and incorporated into larger surfaces. The value of Minimal Mapping Unit (MMU) was 10 pixel diameter. Smaller surfaces were not taken into account. During the vectorization, a more manageable file was generated then generalized with fewer node-points.

Vectorization

Two possibilities were considered to create the borderline of the red mud-covered areas with ENVI 4.8 or ERDAS IMAGINE 2011 software. The advantage of the former is its .HDR format containing the information from the training areas: which part of the image is mud-covered. Thus the vectorization is accomplished by using this information. Completing the vectorization, each object has become determined as an area type resulting in a polygon-type shapefile.

Post-production of vectors

The result of the classification, the vectorgraphic file requires manual corrections. For example the red hues of roofs, ploughlands, withering plants are similar to the mud's red hue.

The corrections of the vectorgraphic file and the evaluation of the statistics were performed by GlobalMapper 13.2 software.

By visual interpretation, the largest extension of the red mud suffusion was located on 5 944 262 m^2 area (100%). The result of the classification was 5 785 793 m^2. The difference between the two methods is 158 469 m^2, which corresponds to 2.67% difference from the visual interpretation.

The typical failures of classification and visual interpretation, and the causes of the difference are the followings:

The semi-automatic classification – although it decreases the subjective effects of the analysis – subtracts the crown and the shadow of the woody plants from the flooded region. The same phenomenon was observed in the areas where gypsum - which had been used to neutralize the alkaline mud – has been washed into the mud. In the affected area trees, shadows, roofs and other incorrectly classified spots outside the flood must be added to or subtracted from the polygon of the flooded area.

During visual interpretation the traces of the mud on gently sloping areas were not considered where the flood has passed through during the first day and painted the vegetation red. This is caused by the subjectivity of the analyzer (Fig. 9. illustrates this). However, the algorithm detected and added these outer areas to the resulting polygon too. Therefore the flooded areas ignored by the analyst also have been delimited. The visual interpreter is unable to distinguish the hues correctly, thus the accuracy is variable by region. In contrast, the classification is less subjective, the accuracy is the same for the whole working area, if illumination has not changed and images are cloud shadow-free during the recording.

On Fig. 2. the yellow polygon system indicates the result of the classification and the red polygon system shows the visual interpretation; by classification the size of the suffusion is 30.11% larger on the sample area than by visual interpretation.

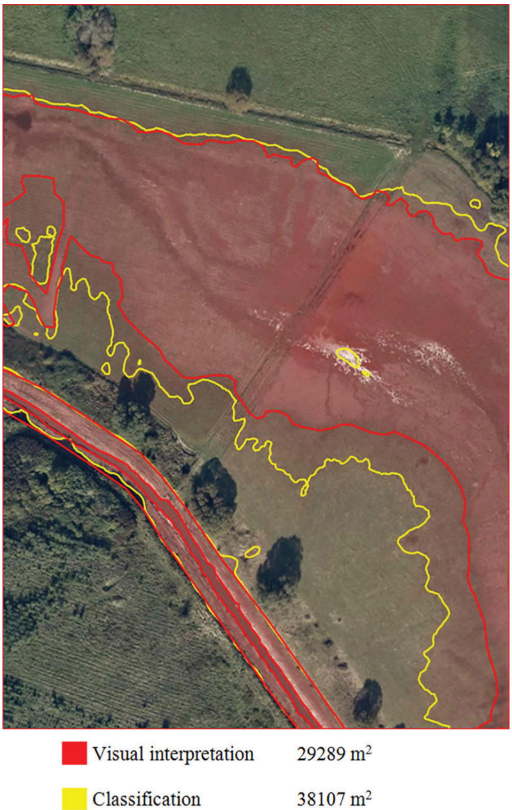

Fig. 9. Differences caused by the subjectivity of the analyzer.

However, in some part of the image map just the opposite could be observed. The classification detected the state of the red mud at the time of the recording, because the receded mud (flooded the area on the preceding days) reflected differently in color and texture in the image. Contrarily, the visual interpretation classified also those sections to the flooded area, where it seemed the mud had been there formerly; for example on the sample area (Fig. 10.) where the mud passed through, but did not accumulate. In similar areas the difference between the classification and the visual interpretation methods is much larger, in this case 81.69%. The result of visual interpretation is 15 573 m^2, the corresponding classification's polygon of the same area is 26 695 m^2. But the size of these sub-areas is minimal; the failures were corrected by vector relocation manually.

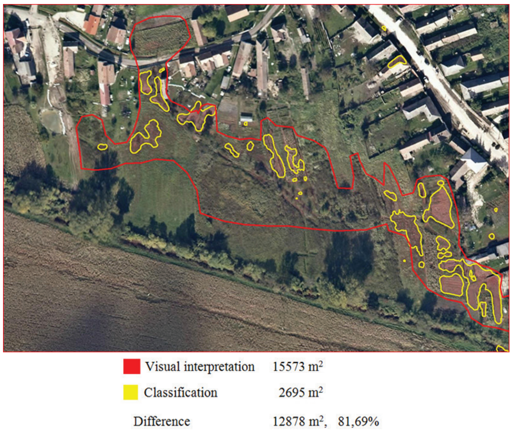

Fig. 10. Visual interpretation classified formerly mudded patches as flooded area

The difference between the objective classification and the subjective visual interpretation method could be verified on surfaces, where the extent of flood has not changed since the mud had passed. These sub-areas usually relate to scarps and terrain representing well the difference between the two interpretational methods.

In this 66 345 m^2 sample area (Fig. 11.) the visual interpretation resulted in 32 630 m2 flooded area, while by classification the result was 32 647 m^2. The 17 m^2 difference corresponds to 0.05% in this case. On Fig. 11. this minimal difference is shown.

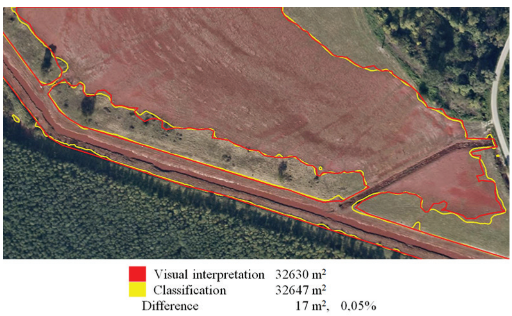

Fig. 11. Difference between the two interpretation methods.

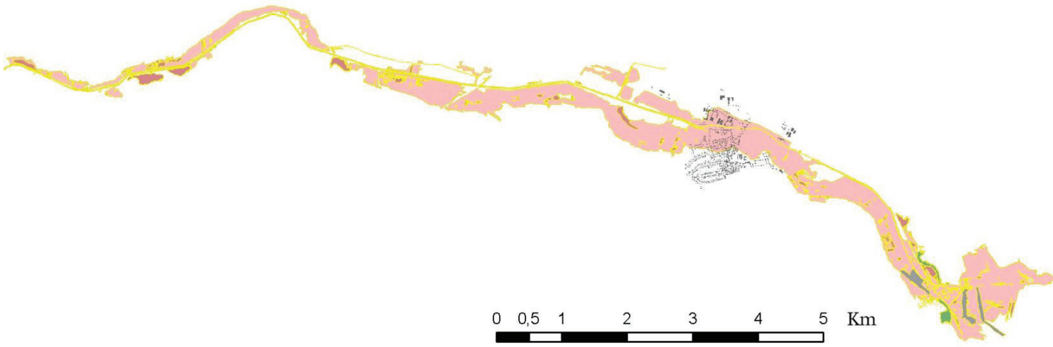

Fig. 12. An overview map of the contaminated area

Figure 13. Flooded part of Kolontár in the geographic information system

3. Results

The area of the stored red mud in the reservoir was 260 514 m^2 before the catastrophe. The amount of the mud can be estimated by using the known parameter of the reservoir. The affected area (except local floods of the streams) is ~ 5 800 000 m^2 (in Kolontár, Devecser, Somlóvásárhely, Somlójenő, Tüskevár and Apácatorna settlements). Inside that area category occurs thicker accumulation zones, where due to the deeper situation of the surface more red mud has been deposited. These areas were inaccessible due to the density and the deepness of the mud. The area of this contamination category is 469 321 m^2. Decreasing the alkalinity, gypsum has been carried out, that sometimes has not been resolved properly; there (on about 23 570 m^2) whitish discoloration and acidic pH appeared, that was also localized with classification. On 11th October the recovery fieldworks have already begun. Till that time the deposited red mud has been removed from 147 322 m^2. On that time 1,285 buildings have stood in Kolontár and Devecser on 238 835 m^2 area (by analyzing the aerial survey with visual interpretation). Among them 450 buildings (on 69 136 m^2 total area) have been affected directly by the flood. This information promotes the estimation of damages as well as the ecologic modeling. The flooded area covered by ligneous vegetation is 411 295 m^2 that means 2 287 groups of trees (by analyzing the aerial survey with classification). An overview map made using the created database seen on Fig. 12. The flooded town of Kolontár is seen on a superposition of aerial image map and vector layer evaluated by visual interpretation. By presenting the disaster-hit area the team has aimed at providing help and drawing attention to the prevention of such industrial disasters. The published data was useful for the disaster management and the emergency management groups working in field (Katasztrofavedelem.hu 2014).

Participants and Acknowledgments

Members of the flight crew: András Arday (pilot), Tamás Lengyel (pilot), Zsolt Molnár (technical leader), Gábor Bakó (aerial camera operator, instrument control engineer)

We would like to thank the members of the photogrammetric group (Gábor Kovács, Gábor Bakó, Zsolt Molnár, Zoltán Eiselt) and the evaluation team's (Béla Licskó - hydrological expert; Krisztina Bálintné Kristóf - radiation protection expert; András Ambrus - evaluation of flooding; Judit Kirisics and Melinda Harsányi - building stock assessment; Tímea Téglási and Ádám Takács - vegetation mapping) voluntary work.

4. References

Bakó, G., 2010. Multispektrális felvételek alapján készülő tematikus térképek minősége, a terepi felbontás és a képminőség függvényében [The quality of thematic maps based on multispectral images depending on spatial resolution and image-quality]. Tájökológiai Lapok, 8 (3), pp. 507-522.

Bakó, G., 2012. Új magyar fejlesztésű szenzorok a légi földmegfigyelés szolgálatában – Egy légi tesztsorozat fázisai [New Hungarian developed sensors serving aerial Earth observation - Stages of an aerial test-series]. AERO, XIV. 2012/2, pp. 20-21.

Bálintné Kirstóf, K. and Bakó G., 2012. Jelenthet-e radioaktív terhelést a vörösiszap? [Could the red mud has radioactive load?]. Természettudományi Közlöny, 143 (3), pp. 134-135.

Burai, P., Samilbegovic, A., Lénárt, Cs., Berkes, J., Milics, G., Tomor, T., Bíró, T., 2011. Preliminary analysis of red mud spill based on aerial imagery. AGD Landscape & Environment, 5 (1), pp. 47-57.

Gelencsér, A., Kováts, N., Turóczi, B., Rostás, Á., Hoffer, A., Imre, K., Nyírő-Kósa, I., Csákberényi-Malasics, D., Tóth, Á., Czitrovszky, A., Nagy, A., Nagy, Sz., Ács, A., Kovács, A., Ferincz, Á., Hartyáni, Zs., Pósafi, M., 2011. The Red MudAccident in Ajka (Hungary): Characterization and Potential Health Effects of Fugitive Dust. Environ. Sci. Technol., 45(4), pp. 1608-1615.

Katasztrofavedelem.hu, 2014. Webpage of the Hungarian Disaster Management Agency.Availablefrom: http://www.katasztrofavedelem.hu/index2.php?pageid=lakossag_kolontar_legifelvetel

Kátai-Urbán, L., Csépő, Z., 2010. Disaster in the Ajka red sludge reservoir on 04 october 2010. 6th Meeting of the Conference of the Parties to the Convention on the Transboundary Effects of Industrial Accidents, The Hague, 8-10 November 2010.

Kvvm.hu, 2011. Kármentesítési útmutató- A felszín alatti vizeket és földtani közeget károsító területhasználatok számbavételének interpretációs kulcsa [Remediation guide - Interpretive key for enumerating the damaging land uses of groundwaters and geological media]. Available from: http://www.kvvm.hu/szakmai/karmentes/kiadvanyok/karmutmutato3/karmutm3-6.htm [Accessed 3 January 2011].

László, I., Ócsai, K., Gera, D. Á., Giachetta, R., Fekete, I., 2011. Object-Based Image Analysis of Pasture with Trees and Red Mud Spill. 31st EARSeL Symposium and 35th General Assembly.

Mta.hu, 2011. Red Sludge Disaster: A Summary of Damage Prevention and the Long-term Interventions, Official homepage of Hungarian Academy of Sciences.Available from: http://mta.hu/news_and_views/red-sludge-disaster-a-summary- of-damage-prevention-and-the-long-term-interventions-126087/ [Accessed 6 August 2011].

Pulford, I. D., Hargreaves, J. S. S., Ďurisová J., Kramulova B., Girad, C., Balakrishnan, M., Barta, V. S., Rico, J. L., 2012. Carbonised red mud – A new water treatment product made from a waste material. Journal of Environmental Management, 100 (15), pp. 59-64.

Ruyters, S., Mertens, J., Vasillieva, A. E., Dehandschutter, B., Poffijn, A., Smolders, E., 2011. The Red Mud Accident in Ajka (Hungary): Plant Toxicity and Trace Metal Bioavailability in Red Mud Contaminated Soil. Environ. Sci. Technol., 45 (4), pp. 1616-1622.

Viczián, I., 2004. Az almásfüzitői vörösiszap zagytározók környezetmorfológiai viszonyai [Environment morphological conditions of red mud reservoirs in Almásfüzitő]. Földrajzi Értesítő,. 53 (1-2), pp. 85-92.